Journal of Statistical Physics, Vol. 125, Nos. 5/6, December 2006 (© 2006)
DOI: 10.1007/s10955-006-9037-7

Domain Patterns in the Microwave-Induced Zero-Resistance State

Ilya Finkler,[1] Bertrand I. Halperin,[1] Assa Auerbach,[2] and Amir Yacoby[3]

Received October 24, 2005; accepted February 3, 2006
Published Online: May 19, 2006

It has been proposed that the microwave-induced "zero-resistance" phenomenon, observed in a GaAs two-dimensional electron system at low temperatures in moderate magnetic fields, results from a state with multiple domains, in which a large local electric field $\mathbf{E}(\mathbf{r})$ is oriented in different directions. We explore here the questions of what may determine the domain arrangement in a given sample, what do the domains look like in representative cases, and what may be the consequences of domain-wall localization on the macroscopic dc conductance. We consider both effects of sample boundaries and effects of disorder, in a simple model, which has a constant Hall conductivity, and is characterized by a Lyapunov functional.

KEY WORDS: quantum Hall effect; two-dimensional electron gas; mesoscopic systems; photoconductivity.

1. INTRODUCTION

The spontaneous formation of domain patterns is a frequent occurrence in nonequilbirium systems, and it has been extensively studied in fluid systems subject to heating or rotation, in nonequilibrium crystal growth, in driven interfaces between immiscible fluids, in roughness patterns on fracture surfaces, in chemically reacting fluids, in dielectric breakdown, in liquid crystal structures, in nonlinear optics, and in motion of granular materials.[1–3] In some cases, domain formation is truly an example of spontaneously broken symmetry, i.e., there are two or more domain structures which are equally possible, and selection between them is triggered by thermal noise or some other accident of the history of the

[1] Physics Laboratories, Harvard University, Cambridge, MA 02138, USA.
[2] Physics Department, Technion, Haifa 32000, Israel.
[3] Department of Physics, Weizmann Institute of Science, Rehovot, Israel.

sample. In other cases, small perturbations due to frozen-in disorder, peculiarities at the boundaries, or other deviations of the physical system from a symmetric idealized model are responsible. In this paper, we discuss a recently discovered system where spontaneous formation of domains is believed to occur and to play an important role in macroscopically observable properties, the so-called microwave-induced zero-resistance state in two-dimensional electron systems, in the presence of a moderately strong magnetic field, at low temperatures.

Experiments on very high mobility two-dimensional electron systems in GaAs heterostructures, in fields ranging from about ten to a few hundred millitesla, have shown large changes in the dc resistance in the presence of microwave radiation, whose sign depends on the ratio $\tilde{\omega} \equiv \omega/\omega_c$ between the microwave frequency ω and the cyclotron frequency ω_c.[4] In particular, decreases in the resistance have been observed when $\tilde{\omega}$ is somewhat larger than the nearest integer. Moreover, in these frequency intervals, if the microwave power is sufficiently high, the resistance can drop by several orders of magnitude, perhaps falling below the experimental sensitivity, whence the designation Zero Resistance State. We note that in the presence of a magnetic field, where there is a nonzero Hall conductance, zero longitudinal resistivity is equivalent to zero longitudinal conductivity: the current is perpendicular to the electric field. Here, we find it more convenient to emphasize the conductivity rather than resistivity. The longitudinal resistance is most directly measured in a Hall bar geometry, whereas the longitudinal conductance is measured in an annular Corbino geometry, illustrated in Fig. 2.

Two distinct microscopic mechanisms for conductivity corrections have been proposed: (i) the displacement photocurrent (DP),[5] which is caused by the photoexcitation of the electrons into displaced guiding centers; and (ii) the distribution

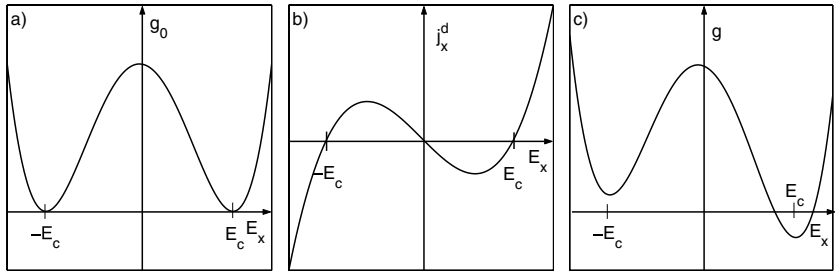

Fig. 1. Model Lyapunov functions g and dissipative current j_x^d for a uniform electrostatic field E_x along the x-axis ($E_y = 0$), in the presence of strong microwave irradiation. (a) Lyapunov function $g_0(E_x)$ in the absence of disorder. Operating points are at the minima of g, where $E_x = \pm E_c$. (b) Dissipative current corresponding to g_0. The dissipative current, parallel to **E**, vanishes at the operating points $E_x = \pm E_c$. There will be a nonzero Hall current in the y-direction. (c) Lyapunov function in the presence of a uniform disorder field $\mathbf{E}_d$ in the x-direction.

function (DF) mechanism, which involves redistribution of intra Landau level population for large inelastic lifetimes.[6]

Andreev *et al.*,[7] have noted that irrespective of microscopic details, once the radiation is strong enough to render the *local* conductivity negative, the system as a whole will break into domains of photogenerated fields and Hall currents. In the proposed domain phase, motion of domain walls can accommodate the external voltage, resulting in a Zero Conductance State (ZCS) in the Corbino geometry, or a Zero Resistance State for the Hall bar geometry, in apparent agreement with experimental reports.[4]

Nevertheless, many questions remain to be answered. What determines the arrangement of domains and domain walls in an actual sample? Is the domain pattern static, or does it evolve periodically or chaotically in time? What are the effects of sample boundaries and inhomogeneities? What do the domain patterns look like in representative cases? If there are favored positions for the domain walls, what effects will this have on the measured electrical conductance?

We address some of these questions here in the framework of a simple phenomenological model. Further details may be found in a previous publication by the current authors.[8]

2. MODEL

2.1. General Form

In our model, in the presence of the microwave field, there is a local, nonlinear relation between the dc current $\mathbf{j}(\mathbf{r})$ and the local electrostatic field $\mathbf{E}(\mathbf{r})$:

$$\mathbf{j} = \mathbf{j}^d(\mathbf{E}, \mathbf{r}) + \mathbf{j}^H(\mathbf{E}, \mathbf{r}), \tag{1}$$

where $\mathbf{j}^H$ is the Hall current and $\mathbf{j}^d$ is the dissipative current, defined by the requirements $\sigma^d_{\alpha\beta} = \sigma^d_{\beta\alpha}$, $\sigma^H_{\alpha\beta} = -\sigma^H_{\beta\alpha}$, where

$$\sigma^d_{\alpha\beta}(\mathbf{E}) \equiv \partial j^d_\alpha / \partial E_\beta, \tag{2}$$

$$\sigma^H_{\alpha\beta}(\mathbf{E}) \equiv \partial j^H_\alpha / \partial E_\beta. \tag{3}$$

These equations must be combined with the continuity equation, $\nabla \cdot \mathbf{j} = -\dot{\rho}$, where ρ is the charge density, and additional equations that relate the electric field to the charge density.

In our simplest model, we assume that the Hall current is given by a linear relation

$$\mathbf{j}^H = \sigma^H \hat{\mathbf{z}} \times \mathbf{E}, \tag{4}$$

and the Hall conductance σ^H is assumed to be a constant, independent of position. As we shall see, there exists a *Lyapunov functional*,[2] which we can use to

determine the steady states, the global conductance, and stability conditions on domain walls in the strong radiation regime.

The function $\mathbf{j}^d$, in general, will depend explicitly on the position $\mathbf{r}$, due, e.g., to inhomogeneities in the 2D electron system, and the direction of $\mathbf{j}^d$ may not be perfectly aligned with $\mathbf{E}$. Equation (1) is valid above an ultraviolet cutoff, which for the system under consideration is probably of the order of the cyclotron radius, of order 1 μm.

Writing $\mathbf{E} \equiv -\nabla\phi$, we may relate changes in the electrostatic potential ϕ to changes in ρ through the inverse capacitance matrix W:

$$\delta\phi(\mathbf{r}) = \int d^2r\, W(\mathbf{r}, \mathbf{r}')\delta\rho(\mathbf{r}'). \tag{5}$$

If a time-independent steady state is reached, then we have simply $\nabla \cdot \mathbf{j} = 0$, and the precise form of W is unimportant.

In a Corbino geometry, one specifies the potential on the inner and outer boundaries of the sample, and one looks for a solution for $\phi(\mathbf{r})$ consistent with these boundary conditions. If σ^H is a constant, then the Hall current cannot contribute to $\nabla \cdot \mathbf{j}$ in the interior of the sample, so it does not appear in Kirchoff's equations. Consequently, the solution for $\phi(\mathbf{r})$ is independent of σ^H, and we may, for simplicity, set $\sigma^H = 0$. To recover the Hall current, one inserts the solution $\mathbf{E}$ into the second term in (1).

The symmetry condition on $\sigma^d_{\alpha\beta}$ allows us to define a Lyapunov functional for $\mathbf{j}^d$, as

$$G[\phi] = \int d^2x g(\mathbf{E}), \quad g = \int_0^{\mathbf{E}(\mathbf{x})} d\mathbf{E}' \cdot \mathbf{j}^d(\mathbf{E}'). \tag{6}$$

A variation of (6) is given by

$$\delta G = \int d^2x \nabla \cdot \mathbf{j}^d\ \delta\phi - \int_{\text{bound}} ds\, \hat{\mathbf{n}} \cdot \mathbf{j}^d \delta\phi. \tag{7}$$

The second integral vanishes on equipotential boundaries, or in the absence of external currents. The extrema of G are found to be steady states, with $\nabla \cdot \mathbf{j} = 0$. Using the positivity of the inverse capacitance matrix W, one may show that $G[\phi(t)]$ is indeed a Lyapunov functional, i.e. a nonincreasing function of time, so that its minima are stable steady states. In general, G may have multiple minima. Any initial choice of $\phi(\mathbf{r})$ will relax to some local minimum of G, but not necessarily the "ground state" with lowest G. It is plausible that minima with higher values of G will tend to have small basins of attraction, and that the system is most likely to end up in a state with G close to the absolute minimum. It is also plausible that, if external noise is present, the system may tend to escape from minima with high values of G, and become trapped near minima with low values of G. In any case, our numerical calculations search for minima with large

basins of attraction (not necessarily the absolute minimum), while the theorems discussed later apply to any local minimum.

Using the boundary term in (7), the current across a Corbino sample is equal to the first derivative of G with respect to the potential difference δV between two edges, and the conductance is given by the stiffness, or the second derivative:

$$\frac{\delta I}{\delta V} = \frac{d^2 G}{d(\delta V)^2}. \tag{8}$$

2.2. Strong Radiation

We now consider the clean system ($\mathbf{E}_d = 0$) in the regime of strong microwave radiation at positive detuning, i.e., with microwave frequencies slightly larger than the cyclotron harmonics $\omega = m\omega_c$, where $m = 1, 2, \ldots$. Both DP and DF mechanisms produce a regime of negative longitudinal conductivity around $E = 0$, which implies a minimum of $g(E)$ at a finite field of magnitude $E = E_c$. If the radiation is strong enough, E_c can become the *global* minimum, and the Lyapunov density describes a dynamical phase of spontaneous photogenerated fields. Then g can be expanded as

$$g_0(\mathbf{E}) = g_0(E_c) + \frac{1}{2}(E - E_c)^2 \sigma_c + \lambda |\nabla \cdot \mathbf{E}|^2, \tag{9}$$

where the subscript 0 denotes the absence of disorder. A representative g and the corresponding dissipative current j^d are shown in Fig. 1a and 1b. To satisfy the equipotential boundary conditions and the constraint $\nabla \times \mathbf{E} = 0$, domain walls between different directions of $\mathbf{E}$ must form. The field derivative coefficient $\lambda \approx \sigma_c l_{dw}^2$ implements the ultraviolet cutoff, giving a finite domain-wall thickness scale l_{dw}. Domain walls give a positive contribution to G of order $\sigma_c E_c^2 l_{dw}$ per unit length. In the absence of disorder, the system will simply minimize this residual domain wall contribution, subject to aforementioned constraints.

Local stability requires that g is concave near E_c. By rotational symmetry g_0 is a "Mexican hat" function with a flat valley along $|\mathbf{E}| = E_c$. Away from domain walls, the fields are "marginally" stable. The clean system has zero conductance in the limit when the system size is much larger than l_{dw}. The system can accommodate a potential difference by moving domain walls and by changing the direction of $\mathbf{E}$ while keeping $|\mathbf{E}| = E_c$, and keeping g_0 constant everywhere away from domain walls. The current density is maintained at zero everywhere, except for possible contributions that vanish in the limit $l_{dw} \to 0$, which is a property of the clean ZCS.[7]

3. DOMAIN STRUCTURE IN THE ABSENCE OF DISORDER

Although the Lyapunov cost per unit length of a domain wall depends on the precise angular difference of the orientations of the electric fields on the two sides of it, the pattern of domain walls in the simplest cases, in the absence of disorder, can be understood as an attempt to minimize the total domain wall length, subject to the boundary constraints. If the potential is a constant, which we may take equal to zero, everywhere along the boundary, we are led to the trial solution:

$$\phi(\mathbf{r}) = E_c d(\mathbf{r}), \tag{10}$$

where $d(\mathbf{r})$ is the distance to the nearest boundary. The negative of this solution, with E_c replaced by $-E_c$, is an equally good solution, with the same Lyaponov cost. Domain walls for these solutions occur along the curves which are the loci of points that are equidistant from two different points on the sample boundary. Domain walls may end, or one domain wall may split into two, at special points, which are equidistant from three different points on the boundary. Some simple examples, illustrating these possibilities, are given in Figs. 2 and 3.

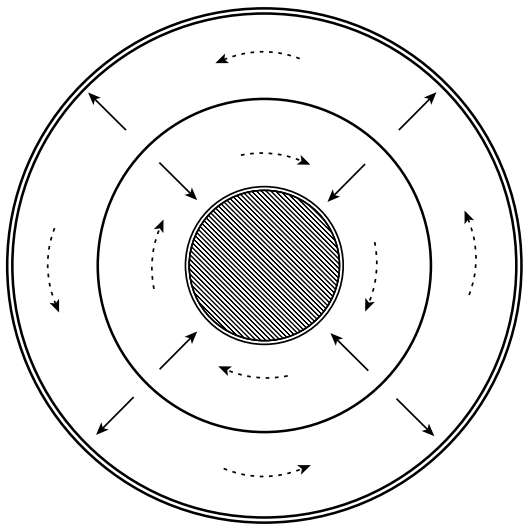

Fig. 2. Domain structure for a circularly symmetric Corbino geometry, in the macroscopic limit, without disorder. *Solid circle*, midway between the inner and outer edges, is the location of the domain wall when there is no voltage difference between the two edges. *Solid arrows* show the direction of the electrostatic field **E**, while *dotted arrows* show the direction of the circulating Hall currents. An alternate solution of the equations has the same position of the domain wall, but reversed directions for the electric fields and Hall currents. In a Corbino conductance measurement, one applies a voltage difference between the inner and the outer edges, and measures the electrical current from one edge to the other.

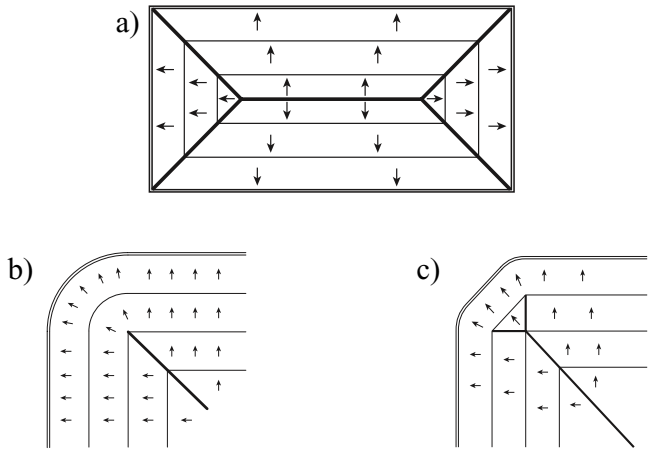

Fig. 3. Other possible domain structures in a sample without disorder. *Heavy solid lines* show domain walls; *light solid lines* show representative equipotential contours; and *double lines* show sample boundaries. *Arrows* show the direction of the electric field **E**. Panel (a) shows the structure for a rectangular sample. Panel (b) shows how a domain wall can end inside the sample, in the vicinity of a curved corner. Panel (c) shows how a domain wall can split into two.

Clearly, the trial solution (10) satisfies the requirement that $E = E_c$ everywhere except on the domain walls. Moreover, the requirement $E = E_c$ requires that in the absence of singularities, two nearby equipotential contours must be separated from each other by a constant distance δ, equal to the difference in the potentials divided by E_c. Thus, if one starts from a point on the sample boundary, the potential $\phi(\mathbf{r})$ must be given by (10) or its negative at least until one encounters a domain wall. If one adds additional domain walls, one may construct solutions different from these, but only by increasing the total length of the domain walls and presumably increasing the Lyapunov cost. Note that one cannot simply displace a domain wall to one side or another without violating the condition $E = E_c$, or introducing a discontinuity in ϕ (i.e., an infinite electric field), which we do not allow.

In the circularly symmetric Corbino geometry, illustrated in Fig. 2, we see that if there is no voltage difference between the inner and outer edges, the domain wall must sit at radius $R = R_m$ where R_m is the arithmetic mean of the radii of the inner and the outer edges. The domain wall has a Lyapunov cost $\delta G = 2\pi R g_w$, where g_w is the cost per unit length of a 180-degree domain wall. If the potential ϕ at the outer edge is increased by a small amount V, while the potential at the inner edge is held constant, the position R of the domain wall must change by an amount $\delta R = \pm V/2E_c$, where the sign depends on which of the two solutions, (10) or its negative, one is starting from. Consequently, since $I = dG/dV$, there

should be a small but nonzero photocurrent, $I = \pm\pi g_w / E_c$ between the outer and the inner edges, at $V = 0$.

Nonzero V breaks the perfect degeneracy between the two steady-state solutions, as the solution with negative δR has the smaller value of G, and it has current in the *opposite* direction to the voltage drop. If the system can switch from one state to another, the current will change direction discontinuously when V passes through zero. In the absence of noise, or if V is changed sufficiently rapidly, however, the system may be trapped in one state or the other, in which case there will be no discontinuity at $V = 0$.

4. LONG WAVELENGTH DISORDER

In an inhomogeneous system, there will generally be a nonzero electrostatic field, $\mathbf{E}_d(\mathbf{r}) \equiv -\nabla\phi_d(\mathbf{r})$ present in the thermal equilibrium state, with no microwave radiation or bias voltage. (Recall that it is the electrochemical potential, which is the sum of the electrostatic potential and the internal chemical potential, that is constant in equilibrium.) We may ask how this disorder field will alter the ZCS.

At weak disorder field, $|\mathbf{E}_d| << E_c$, we expand the Lyapunov density in a region where $E \approx E_c$,

$$g(\mathbf{E}, \mathbf{E}_d) = g_0(\mathbf{E}) - \sigma_1(E)\, \mathbf{E} \cdot \mathbf{E}_d(\mathbf{r}) + \mathcal{O}(E_d^2), \tag{11}$$

which yields a current density

$$\mathbf{j}^d(\mathbf{r}) = -\sigma_1 \mathbf{E}_d + \frac{g_0' - \sigma_1' \mathbf{E} \cdot \mathbf{E}_d}{E} \mathbf{E}, \tag{12}$$

where $X' \equiv \partial X / \partial E$, and the coefficient σ_1 depends on the microscopic mechanism. A typical g in the presence of disorder is displayed in Fig. 1c. For a simple model, based on the displacement mechanism, we estimate that σ_c and $\sigma_1(E_c)$ should be close to the dark conductivity, while $\sigma_1' \ll \sigma_c / E_c$. Other models may have quite different values of σ_1.

Our use of (11) assumes that the length scale of the disorder field is greater than the domain wall thickness l_{dw}, which is the same as our short wavelength cutoff.[9] In practice, however, we will only be interested in fluctuations on length scales much longer than this. In two dimensions, if the disorder potential ϕ_d does not have correlations on a length scale much longer than l_{dw}, and if $E_d \sigma_1 \ll E_c \sigma_c$, then the gain in G obtained by aligning $\mathbf{E}$ with $\mathbf{E}_d$ will be too small to overcome the cost of introducing new domain walls.[8] Then even in the limit of a very large sample, the number and positions of domain walls will be determined by the sample shape and boundary conditions, just as if there were no disorder present. By contrast, if the disorder has correlations which fall off slowly at large distances, then for the model given by (11), with a fixed root-mean-square value of E_d, it

will pay to introduce a network of new domain walls, if the sample is sufficiently large, and we would expect that local characteristics of the domain wall pattern will become independent of the sample size.

4.1. Stability Conditions

Stability requires that the local conductivity tensor σ^d, defined by (2), has nonnegative eigenvalues at every point. The lower (transverse) eigenvalue is given by

$$\sigma_- = \frac{g_0' - \sigma_1' \mathbf{E} \cdot \mathbf{E}_d}{E} + \mathcal{O}(E_d)^2 \geq 0, \tag{13}$$

so marginal stability occurs at $E = E_c + \sigma_1' \mathbf{E}_d \cdot \mathbf{E}/\sigma_c$.

In a steady state, the normal current density across a domain wall must be continuous. If $\hat{\mathbf{n}}$ is the normal, and $\mathbf{E}_1$ and $\mathbf{E}_2$ are the fields on the two sides, we find from (13) and(11) that

$$\sigma_-(E_1)\, \mathbf{E}_1 \cdot \hat{\mathbf{n}} = \sigma_-(E_2)\, \mathbf{E}_2 \cdot \hat{\mathbf{n}} \; + \mathcal{O}(E_{\mathrm{d}}^2), \tag{14}$$

When the normal component of $\mathbf{E}$ has opposite signs on the two sides (as occurs in the clean limit), (14) can only be satisfied for $\sigma_-(E_1) = \sigma_-(E_2) = \mathcal{O}(E_d)^2$. *This restricts the fields at the domain wall to be at their respective marginally stable values*. Among the other consequences of these equations, it can be shown that if a path along a set of domain walls forms a closed loop, the integral of the "two-dimensional disorder-charge density" $q_d(\mathbf{r}) \equiv \nabla \cdot \mathbf{E}_d/2\pi$, over the area enclosed by the loop, must be equal to zero, up to the possible corrections of order E_d^2.[8]

To the lowest order in E_d/E_c, the field $\mathbf{E}$ will have magnitude E_{c} within each domain. Coupled with the fact that the parallel component of electric field is continuous across the domain wall, this implies that the domain wall between any two domains is oriented in such a way as to bisect the angle between the field lines of the two domains.

Finally, we note that generically, the differential conductance of a sample in the Corbino geometry can be obtained by solving for the conductance of a linear system with local conductivity given by $\sigma^d(\mathbf{E}(\mathbf{r}))$, in series with resistive elements along the domain walls, which arise from movement of the domain walls in response to a variation in the applied bias V. There could also be discontinuities in the current at discrete values of V, if the system jumps discontinuously from one minimum of G to another. We find that for weak long-wavelength disorder, the scale of the macroscopic conductance is set by the domain-wall contribution.

4.2. One-Dimensional Disorder

The simplest example to consider is the case of one-dimensional disorder, where ϕ^d is a function of y, independent of the x-coordinate. At wavelengths much larger than l_{dw}, if we do not specify the total voltage drop V, the Lyapunov functional G is minimized if the system breaks up into parallel domains, so that $\mathbf{E}$ is everywhere aligned with $\mathbf{E}_d$, and $\mathbf{j}^d = 0$. These conditions determine $\mathbf{E}(y)$ via (12). They are consistent with the boundary conditions for a rectangular Corbino geometry, which has periodic boundary conditions at $x = 0$ and $x = L$, and specified potentials at $y = 0$ and $y = W$, provided that the voltage difference V satisfies

$$V[I] = \int_0^W dy(E^y(y) - E_d^y(y)). \tag{15}$$

Thus, at strong radiation intensity and zero current, we see that the domain walls form precisely at maxima and minima of ϕ_d, at positions y_i, $i = 1, \ldots, N$, where $E_d^y(y)$ changes sign. For a general choice of $\phi_d(y)$, when no current is drawn from the sample, there will be a nonzero photovoltage, whose value is independent of the magnitude of ϕ_d, to lowest order, and is determined by the positions y_i:

$$V(j = 0) = E_c \left((-1)^N W - 2 \sum_{i=1}^{N} (-1)^i y_i \right) + \mathcal{O}(E_d), \tag{16}$$

where we have assumed that the odd values of i correspond to maxima in ϕ_d.

If there is a nonzero current j_y^d (in the y-direction), the domain walls will be displaced, leading to a change in voltage proportional to j_y^d. For an appropriate choice of j_y^d, such that the voltage resulting from j_y^d cancels the zero-current photovoltage, we can get $V = 0$. Near $j_y^d = 0$, the differential conductivity σ_{yy} is given, to lowest order in ϕ_d, by

$$\frac{1}{\sigma_{yy}} = \frac{2E_c}{\sigma_1 L} \sum_i \frac{1}{|\phi_d''(y_i)|} \equiv \frac{2E_c}{\sigma_1 \tilde{E}_d}. \tag{17}$$

If $P(E_d)$ is the probability distribution for E_d at a random point, it can be shown that $\tilde{E}_d^{-1} = P(0)$. If E_d is taken from a Gaussian distribution, then $\tilde{E}_d = (2\pi)^{1/2} E_d^{\text{rms}}$, where E_d^{rms} is the root-mean-square value of E_d. If ϕ_d is a single sine wave, then $\tilde{E} = 2^{1/2}\pi E_d^{\text{rms}}$. The transverse differential conductivity σ_{xx}, which can also be calculated using (13) and (12), with $j_y^d = 0$, is given, to a first order in ϕ_d, by $\sigma_{xx} = \sigma_d \langle |E_d| \rangle / E_c$, where $\langle |E_d| \rangle$ is the mean value of $|E_d|$. For a Gaussian distribution, one has $\sigma_{xx} = (2/\pi)\sigma_{yy}$, while for a single sine wave, $\sigma_{xx} = (4/\pi^2)\sigma_{yy}$.

In Fig. 4a, we show potentials $\phi(y)$ for the cases $j_y^d = 0$ and $V = 0$, corresponding to a particular choice of the one-dimensional disorder potential $\phi_d(y)$.

4.3. Two-Dimensional Disorder Potentials

4.3.1. Egg-Carton Potential

Perhaps the simplest 2D choice for ϕ_d is the periodic separable egg-carton potential, given by

$$\phi_d = A\sin(k_x x) + B\sin(k_y y). \tag{18}$$

We consider here a finite system, a rectangle L_x by L_y, with periodic boundary conditions on the current and the electric fields. This, of course, is equivalent to considering an infinite system. For bias voltage $V = 0$, we construct a trial solution for ϕ by placing domain walls on the lines $x = \pi(2m+1)/2k_x$ and $y = \pi(2n+1)/2k_y$, for integer n and m. Our trial solution will have a constant electric field in each rectangular domain:

$$\mathbf{E} = E_c(\pm\hat{x}\cos\theta_0 \pm \hat{y}\sin\theta_0). \tag{19}$$

Here, θ_0 is the angle between the field and the y-axis. Combining Eqs. (11) and (19), we see that, to a linear order, minimization of G is equivalent to maximization of $\int d^2x\mathbf{E}\cdot\mathbf{E}_d$. The value of G is minimized with the choice $\theta_0 = \arctan(Ak_x/Bk_y)$. The domain walls satisfy the neutrality condition that $\int q_d(\mathbf{r})d^2r = 0$ in each domain, and the electric field is the gradient of a continuous potential ϕ as required.

In the symmetric case, $k_x = k_y$, $A = B \equiv E_d^0/(2^{1/2}k_x)$, the domain walls form a square array, and $\theta_0 = \pi/4$. We have carried out a numerical minimization

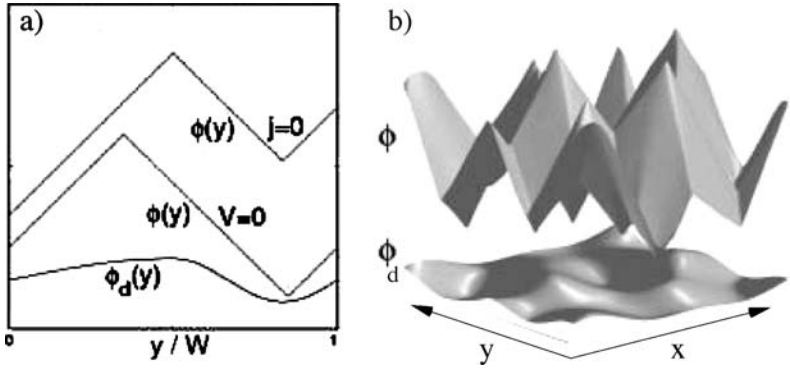

Fig. 4. Examples of a disorder potential $\phi_d(\mathbf{r})$ and the resulting self-consistent potential $\phi(\mathbf{r})$. Different vertical scales were used for ϕ and ϕ_d. Panel (a) shows an example of one-dimensional disorder, where ϕ_d and ϕ depend only on the coordinate y. Solutions are shown for two different boundary conditions, corresponding to zero net voltage drop and to zero longitudinal current flow. Panel (b) shows $\phi(\mathbf{r})$ resulting from a particular two-dimensional disorder potential ϕ_d, indicated in the lower plot. The disorder potential contains 20 Fourier components, whose amplitudes were chosen from Gaussian distributions with variance independent of the wave-vector $\mathbf{k}$. Periodic boundary conditions were imposed on ϕ and ϕ_d.

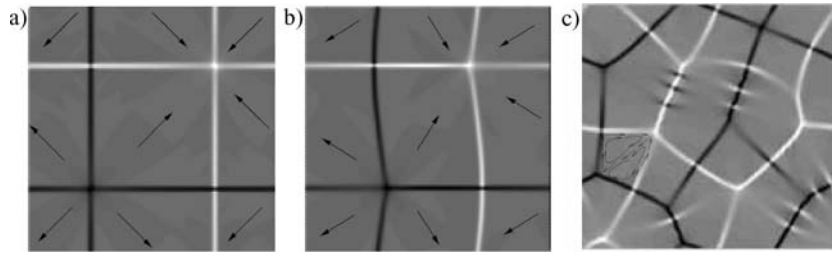

Fig. 5. Gray-scale plots of the "two-dimensional charge density" $q(\mathbf{r}) \equiv \nabla \cdot \mathbf{E}/2\pi$, for three examples discussed in the text. Domain walls are visible as line singularities in the charge density. Panel (a) shows $q(\mathbf{r})$, in one unit cell, when ϕ_d is the periodic symmetric egg-carton potential, $\phi_d \propto \cos x + \cos y$, with zero net voltage drop across the sample. The *arrows* show the direction of electric field within each domain. Panel (b) shows $q(\mathbf{r})$ for the same choice of ϕ_d, with a nonzero voltage bias, corresponding to an average electric field $E = 0.25E_c$ in the x-direction. Once again, the *arrows* show the direction of field within each domain. Panel (c) shows $q(\mathbf{r})$ for the more complicated example of ϕ and ϕ_d illustrated in Fig. 4b. *Arrows* here show circulating dissipative currents in one domain.

of G, and have plotted the "two-dimensional charge density," $q(\mathbf{r}) \equiv \nabla \cdot \mathbf{E}/2\pi$, for the symmetric egg-carton potential, for zero bias voltage in Fig. 5a. Domain walls, appearing here as line singularities, form a square array. Evidently, the numerical solution we obtained is very close to the variational one described previously.

We now construct a variational solution for the case where there is a nonzero voltage drop V along the x-direction. Assuming that the electric field is still constant within each domain, we allow the centers of domain walls that are perpendicular to the voltage drop to shift by amount $\pm\delta x$ and rigidly rotate walls through an angle $\pm\delta\theta$. The electric fields in the various domains will now lie in the directions $\pm(\theta_0 + \delta\theta)$ and $\pm(\pi + \theta_0 - \delta\theta)$, so that the domain walls still bisect the angle formed by the field lines in the neighboring domains. In Fig. 5b, we plot the (numerically obtained) "two-dimensional charge density," for a bias voltage corresponding to an average electric field equal to $0.25E_c$ in the x-direction. The numerical solution is very much like the variational one just described in that domain walls perpendicular to voltage drop are shifted and tilted into a herringbone pattern, while the walls along the voltage drop are essentially unchanged.

The variational solution described previously can be used to evaluate conductivity σ_{xx}. For a voltage drop V along x-direction, we have

$$\frac{2\pi V}{E_c L_x k_x} = 4\delta x \sin\theta_0 + \frac{2\pi}{k_x}\delta\theta \cos\theta_0. \tag{20}$$

Lyapunov functional G will then be

$$G(V) = G_0 + G_1\left(\frac{1}{2}(k_x\delta x)^2 \sin^2\theta_0 + \delta\theta^2\left(\frac{1}{2} + \frac{\pi^2}{24}\left(\frac{k_x}{k_y}\right)^2 \sin^2\theta_0\right)\right), \tag{21}$$

where G_0 is the Lyapunov "energy" for the case of $V = 0$ and $G_1 = (2\sigma_1 E_c L_x L_y)/\pi\sqrt{(Ak_x)^2 + \left(Bk_y\right)^2}$. Using Eq. (20), we minimize the quadratic form above. By taking derivatives of the resulting expression with respect to V, as prescribed by Eq. (8), we obtain the following expression for $\sigma_{xx} = (L_x/L_y)G''(0)$:

$$\sigma_{xx} = \frac{\pi\sigma_1}{2}\,\frac{\sqrt{(Ak_x)^2 + (Bk_y)^2}}{E_c}\,\frac{1 + \frac{\pi^2}{12}\sin^2\theta_0\left(\frac{k_x}{k_y}\right)^2}{1 + \frac{\pi^2}{12}\sin^2\theta_0\left(\frac{k_x}{k_y}\right)^2 + \frac{\pi^2}{4}\cos^2\theta_0}. \tag{22}$$

For the symmetric case, this reduces to $\sigma_{xx} = 0.83\sigma_1 E_d^0/E_c$. As in the 1D case, the conductance is of the order of $\sigma_1 E_d^{\text{rms}}/E_c$, reflecting the pinning effect of the "disorder potential" ϕ_d.

Numerical solutions, referred to earlier, have been obtained by numerically minimizing the Lyapunov functional. We employ a MATLAB-based routine to minimize the functional, which we discretize on a triangular lattice (typically containing around 14,000 points) in order to reduce any perturbations arising from lattice anisotropy. The potential $\phi(\mathbf{r})$ is subject to periodic boundary conditions in the y-direction, and is required to change by a chosen bias voltage V in the x-direction. Having started with a random initial guess for $\phi(\mathbf{r})$, the code allows the potential to relax to a local minimum. The robustness of a minimum, i.e. its "globality," can be ascertained by starting with a different initial guess and/or giving the solution we arrive at random kicks and plugging that in for the next initial guess. As already mentioned, for the case of egg-carton potential, we find that the variational solutions above are quite close to the ones we arrive at via numerics.

4.3.2. Disordered Case

The numerical routine allows us to obtain solutions for disorder potentials much more complicated than the simple egg-carton potential. For example, in Fig. 4b, we display the self-consistent potential $\phi(\mathbf{r})$ for the case of ϕ_d containing 20 Fourier components, chosen from a Gaussian distribution with $\langle|\phi_d(\mathbf{k}|^2\rangle$ independent of $\mathbf{k}$. The disorder potential ϕ_{d} is also shown. In Fig. 5c, we plot the "two-dimensional charge density," proportional to $\nabla \cdot \mathbf{E}$, corresponding to this solution. Domain walls again appear as line singularities in the charge. Although one might expect frustration to reduce the conductance in complicated potentials, the conductivity in this case was found to be similar to that for an egg-carton potential with the same value of E_d^{rms}.

In both the egg-carton potential and the more complicated potential of Fig. 4b, there is frustration in the minimization of G. The field $\mathbf{E}$ is unable to align perfectly with $\mathbf{E}_d(\mathbf{r})$, because of the conflicting requirement of $E \geq E_c$,

which arises from stability, and $\nabla \times \mathbf{E} = 0$. Because of this, the dissipative current j^d is generally nonzero, of order $\sigma_1 E_{\rm d}$, leading to circulating dissipative currents within each domain. These are indicated by arrows for one domain in Fig. 5c. The much larger circulating Hall currents, of magnitude $\sigma^H E_c$, are not shown in the figures.

5. DISCUSSION

In this paper, we have explored the effects of sample boundaries and long-wavelength potential disorder, on the domain pattern and conductance of the microwave-induced zero-resistance state, within a simple model. In particular, our model, with a constant Hall conductance, has the simplifying feature that it has a Lyapunov functional. In considering the effects of disorder, we assumed a linear coupling to the disorder-induced electrostatic field $\mathbf{E}_d$. Furthermore, while we consider nonlinear effects due to the self-consistent electric field $\mathbf{E}$, we do not consider nonlinearities due to changes in the local electron-density itself, which may result from the electric fields of the domains. (We might expect density fluctuations to be small, while potential fluctuations are large, if the system is far from any screening conductors.) For more complicated systems, where there is no Lyapunov functional, we do not even know whether the system will reach a time-independent steady state, in the presence of strong microwave radiation.

Even for our simple model, with its Lyapunov functional G, there are many questions to be answered. What actually is the behavior of a system with two-dimensional disorder, in the limit of a large system size? Will there be a large number of metastable steady states, as in a glass, with associated hysteresis in the observed current/voltage curve? If we assume that for all values of the potential difference V between the inner and the outer edge, in the Corbino geometry, the system can reach the state with the lowest value of G, will the conductance be finite in the limit of large system size, with magnitude of disorder held fixed, or will it, perhaps, go to zero in this limit?

Experimental work in the field is also in its infancy. The self-consistent electrostatic potential $\phi(\mathbf{r})$ generated by the domains can, in principle, be measured with minimal disturbance of the sample, using, for example, a single electron transistor device. Such a method has been used successfully to explore various aspects of the microscopic properties of the integer and fractional quantum Hall effect,[10] and we may expect important information about domain structures to come from such measurements in the future.

We remark that Alicea *et al.*[11] have shown that a Lyapunov functional exists, rather generally, very close to the dynamical phase transition, where the microwave power is such that the longitudinal conductivity first becomes negative at $E = 0$. However, the form of their functional is different from the one employed in the present paper. We are interested here in systems under strong microwave

irradiation, far from the phase transition, so the Lyapunov functional of Alicea *et al.* does not apply.

ACKNOWLEDGMENTS

We thank M. Lukin, S. Fishman, E. Meron, and Y. Yacoby for helpful discussions. Work was supported in part by the Harvard Center for Imaging and Mesoscale Structures, NSF grant DMR02-33773, US-Israel Binational Science Foundation, Minerva Foundation, and the DFG priority program on Quantum Hall Systems YA111/1-1. One of the authors, AA, also acknowledges the hospitality of Aspen Center for Physics.

REFERENCES

1. J. P. Gollub and J. S. Langer, *Rev. Mod. Phys.* **71**:S396 (1999).
2. M. C. Cross and P. C. Hohenberg, *Rev. Mod. Phys.* **65**:851 (1993).
3. J. S. Langer, *Rev. Mod. Phys.* **52**:1 (1980).
4. R. G. Mani, J. H. Smet, K. von Klitzing, V. Narayanamurti, W. B. Johnson and V. Umansky, *Nature* **420**:646 (2002); M. A. Zudov, R. R. Du, L. N. Pfeiffer and K. W. West, *Phys. Rev. Lett.* **90**:046807 (2003); C. L. Yang, M. A. Zudov, T. A. Knuuttila, R. R. Du, L. N. Pfeiffer and K. W. West, *Phys. Rev. Lett.* **91**:096803 (2003); R. L. Willett, L. N. Pfeiffer and K. W. West, *Phys. Rev. Lett.* **93**:026804 (2004).
5. V. I. Ryzhii, *Fiz. Tverd. Tela* **11**:2577 (1969) [*Sov. Phys. Solid State* **11**:2078 (1970)]; A. Durst, S. Sachdev, N. Read and S. M. Girvin, *Phys. Rev. Lett.* **91**:086803 (2003); P. W. Anderson and W. F. Brinkman, cond-mat/0302129; J. Shi and X. C. Xie, *Phys. Rev. Lett.* **91**:086801.
6. I. A. Dmitriev, A. D. Mirlin and D. G. Polyakov, *Phys. Rev. Lett.* **91**:226802 (2003); I. A. Dmitriev, M. G. Vavilov, I. L. Aleiner, A. D. Mirlin and D. G. Polyakov, *Phys. Rev. B* **71**:115316 (2005).
7. A. V. Andreev, I. L. Aleiner and A. J. Millis, Phys. Rev. Lett. **91**:056803 (2003); M. G. Vavilov and I. L. Aleiner, Phys. Rev. B **69**:035303 (2004).
8. A. Auerbach, I. Finkler, B. I. Halperin and A. Yacoby, *Phys. Rev. Lett.* **94**:196801 (2005).
9. Effects of a periodic potential with wavelength *shorter* than the cyclotron radius have been discussed by J. Dietel, L. I. Glazman, F. W. J. Hekking and F. von Oppen, *Phys. Rev. B* **71**:045329 (2005).
10. S. Ilani, J. Martin, E. Teitelbaum, J. H. Smet, D. Mahalu, V. Umansky and A. Yacoby, *Nature* **427**:328 (2004); J. Martin, S. Ilani, B. Verdene, J. H. Smet, V. Umansky, D. Mahalu, D. Schuh, G. Abstreiter and A. Yacoby, *Science* **305**:980 (2004).
11. J. Alicea, L. Balents, M. P. A. Fisher, A. Paramekanti and L. Radzihovsky, *Phys. Rev. B* **71**:235322 (2005).